

Static analysis and simulation of piston coupled diaphragm for microelectromechanical systems based high sensitive sensors

Mohamad Reza Mahlooji, Javad Koohsorkhi ✉

Department of MEMS/NEMS, Faculty of New Sciences and Technologies, University of Tehran, Tehran 1439957131, Iran
✉ E-mail: Koohsorkhi@ut.ac.ir

Published in Micro & Nano Letters; Received on 12th February 2018; Accepted on 28th February 2018

In this work, a new type of diaphragms called ‘piston coupled diaphragm’ is introduced to use as mechanical structure of sensors and micro-electrostatic actuators. Using the static theory based on Kirchhoff–Love theory of plates, expression of deflection is derived. It is assumed that the connection bar area is rigid and simulation results show accuracy of deflection expression. In order to use piston coupled diaphragm as mechanical structure of sensors, electrical and mechanical sensitivity, dynamic range and linear behaviour of the diaphragm are studied. The results show that by choosing a proper dimension of piston coupled diaphragm, because of increased centre rigidity the mechanical sensitivity will decrease but because of realisation of piston-like movement in mechanical structure electrical sensitivity improved by factor of about three in compression to conventional simple diaphragm with the same dimensions and also minimum detectable pressure is improved and linear behaviour of diaphragm degrades. An expression to describe linear behaviour of diaphragm up to 0.54% error from linear response is derived.

1. Introduction: Microelectromechanical systems (MEMS) sensors are electromechanical sensors with micrometre dimensions which offer less weight and size, lower cost, high reliability and could be integrated with electronic processing circuits to reduce noise during signal transmission [1].

Pressure sensor, accelerometer, gyroscope, thermometer, locator, speedometer, dynamometer, flow-meter are major sensors required in mechanical systems that could be manufactured through MEMS technology [2]. The most frequently used electro-mechanical sensor is pressure sensor [3–6]. In addition, microphones are used for controlling and recording audio, ultrasonic and subsonic signals since they can function similar to pressure sensors. As ultrasonic waves enable manufacturing of different sensors to be used in measuring diverse parameters such as flow rate, speed, distance, angle, temperature and humidity [7–10], these sensors or actuators are doubly significant. The diaphragm is an important part of MEMS mechanical sensors. There are several common types of diaphragm used in the MEMS sensors and actuators such as: simple diaphragm [9, 10], corrugated diaphragm [10] and embossed diaphragm [11].

Here, a new type of diaphragms called ‘piston coupled diaphragms (PCDs)’ is studied. The objectives of this structure are realisation of piston-like movement in mechanical structures, isolation of mechanical part of actuator or electromechanical sensors from their electrical part which offer major advantages. This structure offers advantages like independency of mechanical and electrical specifications of diaphragms as well as enhanced sensitivity. In addition, due to piston-like movement of diaphragm and independence design of electrode dimensions, by using this structure could design sensors with high electrical sensitivity and through potentials of this structure could increase dynamic range and decrease low threshold. Based on unique advantages of this structure, it is suitable to use in high sensitive MEMS devices. Furthermore, in this Letter, the structure is analysed from static viewpoint and its deflection formula is developed and sensitivity and linearity range of the structure are determined.

2. Deflection for PCD: Fig. 1 shows the PCD (Fig. 1a) and the structure of PCD-based sensors (Fig. 1b). As shown in this figure, the PCD is made of two parts. The first part is associated with mechanical parameters and called ‘diaphragm’ deflected by pressure while the second part deals with electrical parameters

called suspended electrode acted as a plate of parallel plate capacitor. The primary advantage of this structure is realising piston movement and also isolation of electrical part from mechanical.

From static viewpoint, the two problems should be considered in the present design. First, increased thickness of centre of diaphragm leads to enhanced rigidity of diaphragm and reduced mechanical sensitivity. The second problem is the mass connected to central point of diaphragm which generates initial deflection within diaphragm. In order to deal with these two problems, it is essential to develop a proper formula for deflection of this diaphragm. The structure and dimensional parameters of PCD are represented in Fig. 1 and Table 1, respectively.

In the case that deflection of plate against its thickness is small, deflection of plate follows the general expression below [12]:

$$\nabla^4 w = P \quad (1)$$

where P is pressure and w is deflection. If circular plate has a symmetrical loading, (1) could be simplified to the following manner [12]:

$$\frac{d}{dr} \left[\frac{1}{r} \frac{d}{dr} \left(r \frac{dw}{dr} \right) \right] = -\frac{Q_r}{D} \quad (2)$$

Here, D refers to flexural stiffness of the plate defined as [12]

$$D = \frac{Et^3}{12(1-\nu^2)} \quad (3)$$

where E refers to Young’s modulus, t is the thickness of the plate and ν represents Poisson’s ratio. Solving the above differential equation should be done based on expression (4) and its coefficients are determined by applying boundary conditions [12]

$$w = \frac{C_1}{4} r^2 + C_2 \ln r + C_3 + \frac{P}{64D} r^4 \quad (4)$$

As the surface of PCD has two thickness levels at connection area and its surrounding, as shown in Fig. 1, two expressions will be developed for analysis of PCD. The expressions consider dimensional status of the parts and it is assumed that the central part is completely rigid. The rigidity of the area implies that the ratio of height to radius is so high that the whole central area of beam connection will have identical deflection. Then, deflection gradient of

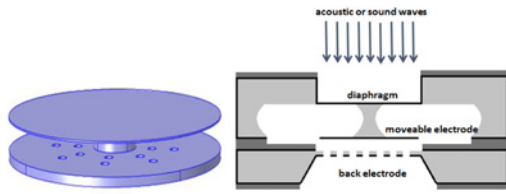


Fig. 1 Schematic diagram of PCD-based sensor
a PCD, **b** Structure of sensor using the two processed silicon wafers bonded together

Table 1 Dimensions of simulated structure

Parameter	Symbol	Parameter	Symbol
diaphragm radius	a	air gap	g
bar radius	b	diaphragm area	A_d
electrode radius	c	bar area	A_b
diaphragm thickness	ta	electrode area	A_e
bar thickness	h	hole electrode radius	$r_{h,e}$
electrode thickness	tc	hole radius of back plate	$r_{h,b}$

Table 2 Boundary condition

$w_2(r = a) = 0$	boundary condition of clamped edge
$w_2'(r = a) = 0$	boundary condition of clamped edge
$w_1(r = b) = CR$	boundary condition of connecting edge
$w_1'(r = b) = 0$	boundary condition of connecting edge

the whole connection area will be zero. Regarding expression for the second part, boundary conditions at the radius b and clamped margins are consequently detailed in Table 2. Applying uniform pressure P on surface of diaphragm and considering boundary conditions as detailed in Table 2, deflection expression of PCD will be derived as below:

$$w_1 = C_R, \quad 0 < r < b$$

$$w_2 = \frac{C_{r12}}{4}r^2 + C_{r22}\ln r + C_{r32} + \frac{P}{64D}r^4, \quad b < r < a \quad (5)$$

$$C_R = P \frac{a^4}{64D_e} \left(1 - \frac{b^4}{a^4} + 4 \frac{b^2}{a^2} \ln \left(\frac{b}{a} \right) \right), \quad D_e = \frac{Eh^3}{12(1-\nu^2)} \quad (6)$$

$$C_{r12} = -P \frac{a^2}{8D} \left(1 + \frac{b^2}{a^2} \right) \quad (7)$$

$$C_{r22} = P \frac{a^2 b^2}{16D} \quad (8)$$

$$C_{r32} = P \frac{a^4}{64D} \left(1 - 2 \frac{b^2}{a^2} - 4 \frac{b^2}{a^2} \ln(a) \right) \quad (9)$$

Fig. 2 shows the effect of different diaphragm thickness in deflection of PCD. As shown in this figure, the simulation results and data from the derived equation are in good agreement.

As shown in Fig. 3, the assumption of rigid centre is accurate if the height, h , will be sufficiently long.

3. Sensitivity

3.1. Mechanical sensitivity: Mechanical sensitivity is defined as the ratio of change in measurable mechanical parameter to input parameter of the system. The measurable parameter is displacement or deflection in capacitive mechanism. The whole deflection of centre of PCD is transmitted to suspended electrode. Therefore, mechanical sensitivity (i.e. S_m) is ratio of deflection of

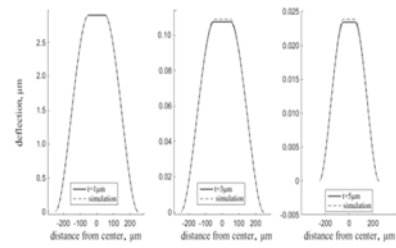


Fig. 2 Deflection a long PCD diameter for different thickness

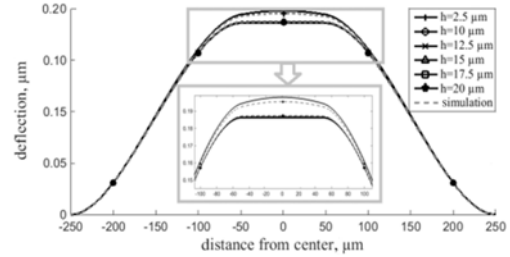


Fig. 3 Deflection along length for different height of bar comparison of derived equation versus the simulation results with rigid embossment region

PCD centre part to applied pressure

$$S_{m,PCD} = \frac{a^4}{64D} \left(1 - \frac{b^4}{a^4} + 4 \frac{b^2}{a^2} \ln \left(\frac{b}{a} \right) \right) \quad (10)$$

$$= S_{m,s} \left(1 - \frac{b^4}{a^4} + 4 \frac{b^2}{a^2} \ln \left(\frac{b}{a} \right) \right)$$

where $S_{m,PCD}$ and $S_{m,s}$ are mechanical sensitivity of PCD and simple diaphragm, respectively. As shown above, in comparison with simple diaphragm the mechanical sensitivity of PCD will reduce as b/a ratio increased. Due to rigidity of the centre, deflection and mechanical sensitivity of the structure will be lower than simple counterpart.

3.2. Electrical sensitivity: Electrical sensitivity is defined as variation of capacitance in relation to deflection of the structure. Under influence of input pressure, electrical sensitivity causes deflection of diaphragm, change of air gap between electrodes of capacitive plates and change of capacitance

$$C = \frac{\epsilon \cdot A_e}{g} = \frac{\epsilon \cdot A_e}{g_0 - w_1} \quad (11)$$

where C , ϵ , A_e , g , g_0 and w_1 are capacitance, permittivity, electrode area, gap between two electrodes, initial gap and deflection, respectively. Considering constant voltage mode, the charge of capacitor will be

$$Q = C \cdot V = \frac{\epsilon \cdot A_e}{g_0 - w_1} \cdot V \quad (12)$$

$$\Delta Q(t) = \frac{\epsilon \cdot A_e}{g_0} V - \frac{\epsilon \cdot A_e}{g_0 - w_1} V = - \frac{\epsilon \cdot A_e}{g_0} \frac{w_1}{g_0 - w_1} V \quad (13)$$

$$= -C_0 \frac{w_1}{g_0 - w_1} V_0 = -\Delta C V_0$$

where Q , V , C_0 are charge, bias voltage and initial capacitance, respectively. Variation of capacitance is nonlinear associated with deflection of diaphragm or air gap and this is deemed to be undesirable from viewpoint of sensing reading. Therefore, variation of capacitance is approximately turned linear as shown

in the following:

$$\Delta C = C_0 \frac{w_1}{g_0 - w_1} \frac{g_0 + w_1}{g_0 + w_1} = C_0 \frac{g_0 w_1 + w_1^2}{g_0^2 - w_1^2} \quad (14)$$

If deflection of diaphragm is small in comparison with initial air gap (e.g. 0.1), w_1^2 will be negligible. Consequently, above expression will be simplified to the following expression which is linearly associated with deflection of diaphragm

$$\Delta C = C_0 \frac{w_1}{g_0} \quad (15)$$

In the case of simple diaphragm, capacitance of all differential elements of capacitors will be equal with [13]

$$\begin{aligned} dc &= C_0 \frac{dQ}{-(\sigma/\epsilon_0)g(r) ds} = \frac{dQ}{-(\sigma/\epsilon_0)g(r)} = \frac{\sigma dA}{-(\sigma/\epsilon_0)g(r)} \\ &= \frac{\epsilon_0 dA}{g(r)} \end{aligned} \quad (16)$$

Due to the fact that air gap denotes initial air gap and deflection of diaphragm, in the case of considering deflection of simple diaphragm, its total capacitance will be shown as below:

$$c = \int_0^a \frac{2\pi\epsilon_0 r}{g_0 - w(0)(1 - ((r/a))^2)^2} dr \quad (17)$$

where $w(0)$ is centre deflection of diaphragm. After analytical solution of expression (17), the integral solution will be as shown in the following [14]:

$$|c| = \begin{cases} \frac{\operatorname{arctanh}\sqrt{(w(0)/g_0)} \epsilon_0 \pi a^2}{(w(0)/g_0) g_0}, & w(0) \geq 0 \\ \frac{\operatorname{arctan}\sqrt{-(w(0)/g_0)} \epsilon_0 \pi a^2}{-(w(0)/g_0) g_0}, & w(0) \leq 0 \end{cases} \quad (18)$$

In the case that deflection is <20% of air gap, above expression will be as shown in the following after extending Taylor series with <1% error

$$\operatorname{arctan} hx = x + \frac{x^3}{3} \quad \text{and} \quad \operatorname{arctan} x = x - \frac{x^3}{3} \quad (19)$$

$$C_{\text{eff}} = \frac{\epsilon_0 A}{g_0} \left(1 + \frac{1}{3} \frac{w_0}{g_0}\right) \quad (20)$$

If variation of capacitance is considered as suggested in expression (16), changes of effective capacitance for simple diaphragm will be

$$\Delta C_{\text{eff}} = \frac{1}{3} \frac{w_0}{g_0} \frac{\epsilon_0 A}{g_0 - w_0} = \frac{1}{3} C_0 \frac{w_0}{g_0} \quad (21)$$

$$\Delta C_{\text{eff,PCD}} = C_0 \frac{w_0}{g_0}$$

3.3. Total sensitivity: Total sensitivity is the final product of multiplication of mechanical sensitivity by electrical sensitivity. For simple and PCD, total sensitivity, S , is, respectively, equivalent to

$$\frac{\Delta C_{\text{eff}}}{P} = \frac{1}{3} \frac{C_0}{g_0} N_f = \frac{1}{3} \frac{C_0}{g_0} \frac{a^4}{64D} \quad (22)$$

$$\frac{\Delta C}{P} = \frac{C_0}{g_0} N_u = \frac{C_0}{g_0} \cdot \frac{a^4}{64D} \left(1 - \frac{b^4}{a^4} + 4 \frac{b^2}{a^2} \ln\left(\frac{b}{a}\right)\right) \quad (23)$$

where N_s and N_{PCD} are the centre deflection of simple diaphragm and PCD, respectively. The above value is one-third of cylindrical form of PCD. Consequently, if dimensions of electrode in PCD are $(\sqrt{3}/3)$ smaller than that of simple

diaphragm the use of PCD will not have advantage over the use of simple one. Maximum b/a ratio of PCD to make it superior to simple diaphragm are obtained as

$$\begin{aligned} \frac{\Delta C_{\text{eff}}}{P} (\text{simple}) &= \frac{\Delta C}{P} (\text{PCD}) \rightarrow \frac{1}{3} \frac{\epsilon_0 a^2}{g_0} \cdot \frac{a^4}{64D} \\ &= \frac{\epsilon_0 c^2}{g_0} \cdot \frac{a^4}{64D} \left(1 - \frac{b^4}{a^4} + 4 \frac{b^2}{a^2} \ln\left(\frac{b}{a}\right)\right) \frac{1}{3} \frac{a^4}{c^2} \quad (24) \\ &= 1 - \frac{b^4}{a^4} + 4 \frac{b^2}{a^2} \ln\left(\frac{b}{a}\right) \end{aligned}$$

Assuming $a = c$, critical b/a ratio will be equal to 0.435. Simulation results and total sensitivity by applying 1 Pa pressure for different b/a ratios and a radius are represented in Fig. 4. Dashed line shows sensitivity of simple diaphragm and determines b/a ratio of 0.44 which supports the accuracy of above expressions. If b/a ratio is <0.44 and the area of c electrode is equal to area of a diaphragm, the PCD shows higher sensitivity than simple one. However, in the case of larger b , increasing radius of electrodes could compensate for comparatively less sensitivity of PCD.

Variations of capacitance should be measured by changes in circuit excitement parameters, current or voltage. Therefore, capacitor should be biased either through applying fixed charge on the electrode or through applying fixed voltage between two electrodes. In both cases, there is a potential difference between two electrodes which should be less than pull-in voltage. Otherwise, the structure leads to static instability and the two electrodes fall on each other

$$S = V_{\text{pull in}} \frac{C_0}{g_0} N \quad (25)$$

where N and $V_{\text{pull in}}$ are the centre deflection per unit pressure level and pull-in voltage, respectively. Since pull-in voltage of simple and PCD are obtained, respectively, as

$$V_{\text{pull in/simple}} = \sqrt{\frac{8}{27} \frac{g_0^3}{\epsilon_0 N_f}} = \sqrt{\frac{8}{27} \frac{g_0^2 A_a}{C_0 N_f}} \quad (26)$$

$$V_{\text{pull in/PCD}} = \sqrt{\frac{8}{27} \frac{A_b g_0^3}{\epsilon_0 A_e N_c}} = \sqrt{\frac{8}{27} \frac{g_0^2 A_b}{C_0 N_c}} \quad (27)$$

where A_a and A_b and A_e are area of diaphragm, bar, and electrode, respectively, and N_c is centre deflection of PCD which the loading is applied to electrode due to electrostatic loading and transmitted to the bar area. Then, putting (27) into (25) and considering (2) which shows coefficient N_{PCD} , maximum total sensitivity of PCD is

$$S_{\text{PCD}} = V_{\text{pull in}} \frac{C_0}{g_0} N_{\text{PCD}} = \sqrt{\frac{8}{27} C_0 A_b \frac{N_{\text{PCD}}^2}{N_c}} \quad (28)$$

The above expression points to some facts. First, higher initial capacitance is associated with higher sensitivity. Second, lower air gap

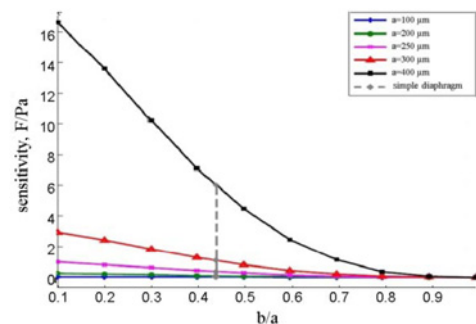


Fig. 4 Sensitivity of PCD versus pressure for different bar radius

is associated with higher sensitivity. Third, more flexible diaphragm is correlated with higher sensitivity. The maximum sensitivity ratio of PCD to simple one is equal to

(see equation (29))

As shown in (29), if connection radius of beam is zero (i.e. $b=0$) and radius of electrode and diaphragm is identical (i.e. $c=a$), sensitivity of PCD will not be three times higher than that of simple diaphragm despite of the expectation one has of (22). The reason behind this issue is applying electrostatic force on the centre of diaphragm (i.e. most flexible part of diaphragm) and reduced pull-in voltage. Capacitance variations of simple diaphragms are much less than PCDs.

The mechanical and electrical sensitivity of simple diaphragm is not linear. This signifies that as pressure increases, sensitivity will not be constant but will decline. Clamped boundary conditions lead to nonlinear effects. Addition of central embossment will contribute to a nonlinear association. Consequently, higher radius of embossment will be associated with higher nonlinearity due to reduced less-thick area around the embossment. Therefore, initial deflection of diaphragms could contribute to reduced sensitivity. With regard to simple diaphragm, electrical sensitivity is more linear than PCD because electric sensitivity is directly associated with deflection of diaphragm due to air gap. Evidently, capacitance of simple diaphragm in margins of its plate changes in response to smaller deflection. Therefore, it is regarded as small deflection in the presumed theoretical range. Considering PCD, total deflection at the centre of diaphragm is transmitted to the whole surface of electrode. In fact, deflection of the whole electrode surface enters a larger theoretical range of deflection. This means that level of nonlinear deflection is multiplied by coefficient of the whole electrode surface and this leads to increase nonlinearity.

Electrostatic force and weight force attached to the centre of the diaphragm are primary factors of initial deflection or displacement. The force is applied to central area of connection point. As the whole force is applied on a small surface, the level of deflection could be large. The initial force might be

$$P_{\text{frist}} = \frac{F_{\text{elec}} + F_w}{A_b} \quad (30)$$

$$F_w = \rho V_{\text{volum}} = \rho(\pi b^2 h + \pi c^2 t_e - N \pi r_h^2 t_e)g \quad (31)$$

For example, if one presumes a silicon-made diaphragm with density of 2230 kg/m^3 and dimensions of $a=250$, $b=50$ and $h=30 \mu\text{m}$, the weight force applied on the diaphragm will be equivalent with

$$\begin{aligned} F_w &= \rho V_{\text{volum}}g = 2230(\pi \times 50^2 \times 30 + \pi \times 250^2 \times 10)10^{-18} \times 10 \\ &= 0.049 \times 10^{-6} = 0.049 \mu\text{N} \rightarrow P_w = \frac{F_w}{A_b} \\ &= \frac{0.049 \mu\text{N}}{\pi \times 50^2 \times 10^{-12}} = 6.24 \text{ Pa} \end{aligned} \quad (32)$$

Presuming voltage bias of 20 V, air gap of $2 \mu\text{m}$ and equal surface of electrode and diaphragm, electrostatic force of the sample will be

equal with

$$\begin{aligned} F_{\text{elec}} &= \frac{1}{2} \frac{\epsilon_0 A_e}{(g_0 - x)^2} V^2 = \frac{1}{2} \pi \frac{8.854 \times 10^{-14} \times 250^2 \times 10^{-12}}{2^2 \times 10^{-12}} 20^2 \\ &= 0.0086 \mu\text{N} \rightarrow P_{\text{elec}} = \frac{0.0086 \mu\text{N}}{\pi \times 50^2 \times 10^{-12}} = 1.01 \text{ Pa} \end{aligned} \quad (33)$$

Through simulation, one could observe that the displacement under 10 Pa and below is within the range of tens of nanometres. If one desires to design a diaphragm for measuring internal pressures the air gap is within micrometres range, therefore initial displacement due to application of these forces could be neglected. However, there are some facts to be noted. First, if designer intends to measure very low pressures (down to millipascal) the displacement should be considered. Otherwise, measurement error will be significant. Second, increased radius of diaphragm adds to flexibility of diaphragm. In addition, increased surface of diaphragm adds to electrostatic force and consequently, initial deflection will be significant. Electric sensitivity is also due to inverse association of capacitance with nonlinear air gap. Finally, output of MEMS part (i.e. voltage) could be determined from expression (36)

$$\Delta C = C_0 \frac{w(t)}{g_0} = \frac{C_0 P(t)}{g_0 T} \quad (34)$$

$$\begin{aligned} V_{\text{out}} &= G_{\text{IC}}(V_b) \cdot \Delta C = \frac{C_0 P(t)}{g_0 T} \rightarrow S = G_{\text{IC}}(V_b) \cdot \frac{C_0}{T \cdot g_0} \\ &= G_{\text{IC}} \cdot G_{\text{MEMS}} \end{aligned} \quad (35)$$

Figs. 5 and 6 show simulation results of sensitivity of simple and PCDs. Fig. 5 shows sensitivity, i.e. $(\Delta C/P)$, in respect of pressures for different radius of bar. It is assumed that dimension of electrode is equal to those of diaphragm.

Based on these figure, there are some noteworthy points. First, electric sensitivity rises as pressure increases while mechanical sensitivity reduces as pressure rises. This is due to nonlinear association of capacitance variations with air gap. This implies an inverse association between capacitance and squared air gap. Second, increase of b is followed by reducing sensitivity and this event is due to reduced mechanical sensitivity. Choosing b up to 40% of diaphragm radius makes general sensitivity of PCD more than simple diaphragm with the same dimensions. This suggests that piston-like movement of electrode could properly compensate the reduced rigidity-caused mechanical sensitivity at the centre of diaphragm with b radius.

In fact, sensitivity is a coefficient of bias voltage. Higher voltage bias is correlated with higher sensitivity. Fig. 6 shows maximum sensitivity for different b values. This implies that the limitation that increase of sensitivity leads concurrently to reduced pull-in voltage has also been considered. Observably, pull-in phenomenon influences sensitivity of output significantly.

4. Dynamic range: The ratio of specified maximum level of a parameter to minimum detectable value of that parameter is defined as dynamic range [2]. The readout circuit limits the minimum detectable pressure due to minimum noiseless capacitance which could be sensed (i.e. 4 aF) that initial capacitance and mechanical sensitivity of diaphragm introduce variation of capacitance. In terms of high threshold, more factors

$$\begin{aligned} \frac{S_{\text{couple}}}{S_{\text{simple}}} &= 3 \sqrt{\frac{A_c A_b N_{\text{PCD}}^2}{A_a A_a N_s N_c}} \\ &= \frac{3c}{2a} \sqrt{\frac{(1 - (b^2/a^2))}{(1 - 2(b^2/a^2)(2 \ln(ab)^2 - 4 \ln(a) \ln(b) + 1) + (b^4/a^4) * (1 - (b^4/a^4) + 4(b^2/a^2) \ln((b/a)))}} \end{aligned} \quad (29)$$

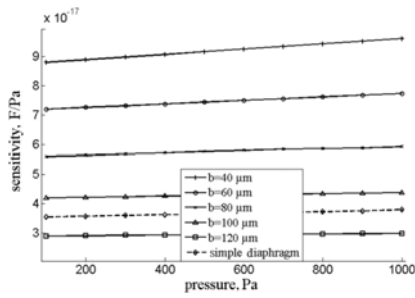


Fig. 5 Sensitivity of PCD in b/a ratio for different diaphragm radius and compared with simple diaphragm

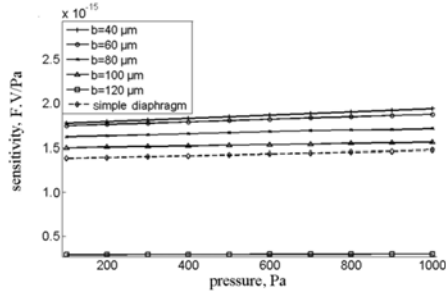


Fig. 6 Maximum accessible sensitivity considering maximum biasing voltage

are involved such as entry of material to plastic zone or its failure, exceeding deflection of diaphragm from theoretical limit of small deflection, start of nonlinear expression for diaphragm, exceeding of diaphragm's deflection from the range in which expression for variation of capacitance is linear, exceeding of electrode from one-third of air gap and occurrence of pull-in phenomenon in which fall suspended electrode on rear electrode. Minimal measurable pressure through reading circuit is determined based on minimum measurable deflection

$$P_{\min} = CR \cdot w_{\min} \quad (36)$$

Considering expression (14), minimum value of required deflection will be obtained

$$w_{\min} = d - \frac{\epsilon_0 A_e}{(\Delta C_{\min} + (\epsilon_0 A_e/d))} \quad (37)$$

Based on PCap02 IC, ΔC_{\min} is considered to be 4 aF. As shown in Fig. 7, low threshold of pressure detectable through microphone, based on b/a ratio for different radii of diaphragm and in comparison with low threshold pressure of simple diaphragm is highlighted by dashed line. In the figure, it is evident that if b/a ratio exceed 0.44, low threshold of PCD will be worse than simple diaphragm.

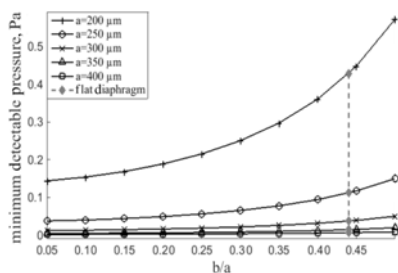


Fig. 7 Minimum detectable pressure of PCD for different b/a ratio

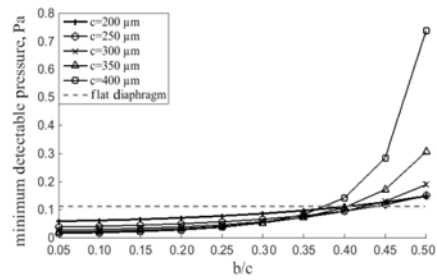


Fig. 8 Minimum detectable pressure of PCD for different b/c ratio

The advantage of PCD is decrease of low threshold down to required level by increasing surface of electrode. This is despite of the fact that b exerts negative influence on flexibility of diaphragm which leads to increase of minimum detectable pressure. Fig. 8 represents low threshold in terms of b/a ratios for different c values. Evidently, increased surface of suspended electrode could reduce low threshold in the case of different millipascal ranges. This issue is highly significant for sensitive sensors. As a result, if a wide dynamic range is intended by designer, could reduce low threshold by increasing surface of electrode. In contrast, reducing surface of diaphragm will increase high threshold.

Another problem to be analysed is behaviour of PCD out of linear response. Deviation from linear state is based on level of error or difference in sensitivity for high pressures compared with lower pressures because the expression for deflection of diaphragm is

$$P = Ay + By^3 \quad (38)$$

In the case of low pressures, the whole work that pressure should do is bending diaphragm and this stores bending strain energy in diaphragm. In the case of high pressures, in addition to the energy to be used for bending diaphragm some energy should be spent for pulling intermediate plate so that diaphragm could provide essential displacement for large deflection. Therefore, some of the work that pressure should do is assigned to stretching middle plate. Therefore, higher pressure adds to the level of required tensile energy and reduces the ratio of pressure to deflection. In the case of designing sensors, linearity of sensing is significant. Therefore, deviation of displacement–pressure ratio in higher pressures compared with displacement–pressure ratio in lower pressures should be regarded as basic principle. During analysis of plates, displacement–pressure ratio is regarded as basic principle and this does not make a difference. In this case, error or deviation could be defined based on the following equation:

$$\text{Error}(\%) = \frac{P - (P/w_{\text{linear}})w_{\text{nonlinear}}}{(P/w_{\text{linear}})w_{\text{nonlinear}}} \quad (39)$$

Based on the above measure, error level is represented in Table 3 for 10 and 25% deflection of thickness. In this regard, different theories for major deflection of simple diaphragm will be drawn upon. The

Table 3 Criterion error of out of linear region in some theory to determine large deflection of diaphragm

Theory	$w/t, \%$	Error, %
Timoshenko and Woinowsky-Krieger [12]	10	0.488
	25	3.05
Bert <i>et al.</i> [3]	10	0.53
	25	3.31
Beeby [15]	10	0.41
	25	2.56

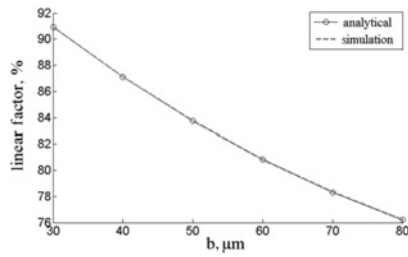


Fig. 9 Deflection to thickness valid ratio with assumption of 0.54% error versus the linear behaviour for different bar radius

results of finite-element simulation support higher accuracy of expression of Bert.

In the case of designing simple diaphragm, deflection per 10% thickness is presumed. In this case, ratio of sentence y^3 (38) to sentence y is 0.53. Regarding PCD, level of error depends on radius b because level of energies will depend on b . If error of simple diaphragm (0.53) is identically regarded as basis for linear range of PCD, error value of 0.53 will occur for those deflections which are <10% of thickness. In order to analyse nonlinear part of pressure–displacement association through simulation results, pressure–displacement ratio (in the case of finite–element linear solution) is regarded as basis for deviation from linear pressure–displacement association. Consequently, simulation data is compared and simulation error is eliminated. The measure of linear range per 10% thickness, defined for simple diaphragm, will be as shown in the following for a PCD. In this case, αt is also called linear deflection. For PCD, this value should be multiplied by variation of strain energies of diaphragm.

Increase of stain energy is associated with quicker entry of diaphragm into nonlinear zone. Therefore, linear deflection is directly associated with bending energy and follows expression (34)

$$(\alpha t)_{\text{couple}} = (\alpha t)_{\text{flat}} \left[\frac{V_{u,\text{flat}}}{V_{u,\text{couple}}} \right] \cdot \left[\frac{V_{w,\text{couple}}}{V_{w,\text{flat}}} \right] \quad (40)$$

Here, αt refers to intended percentage of thickness for simple diaphragm. In designing process, this variable is presumed to be 10%. Strain energy of bending in polar coordinate is obtained by

$$V_w = \frac{D}{2} \int_0^{2\pi} \int_b^a \left[\left(\frac{\partial^2 w}{\partial r^2} \right)^2 + \frac{1}{r^2} \left(\frac{\partial w}{\partial r} \right)^2 + 2 \frac{v}{r} \frac{\partial w}{\partial r} \frac{\partial^2 w}{\partial r^2} \right] r dr d\theta \quad (41)$$

Also the strain energy of middle plane which is stretched is

$$\begin{aligned} V_u &= 2\pi \int_0^b \left(\frac{N_r \varepsilon_r}{2} + \frac{N_t \varepsilon_t}{2} \right) r dr \\ &= \frac{\pi E h}{1 - \nu^2} \int_0^b (\varepsilon_r^2 + \varepsilon_t^2 + 2\nu \varepsilon_r \varepsilon_t) r dr \end{aligned} \quad (42)$$

In which the strain in radial direction and tangential direction are

$$\varepsilon_r = \frac{du}{dr} + \frac{1}{2} \left(\frac{dw}{dr} \right)^2 \quad \text{and} \quad \varepsilon_t = \frac{u}{r} \quad (43)$$

Radial displacement could be explained

$$u = (b - r)(a - r)(d_{12} + d_{22}r + d_{32}r^2 + \dots) \quad (44)$$

In which two first terms are satisfied boundary conditions and the radial displacement should be zero on the clamped and connection edges. The tensile force per unit length in radial and tangential

direction is

$$N_r = \frac{Eh}{1 - \nu^2} (\varepsilon_r + \nu \varepsilon_t) \quad \text{and} \quad N_t = \frac{Eh}{1 - \nu^2} (\varepsilon_t + \nu \varepsilon_r) \quad (45)$$

The total energy of this structure in equilibrium position should be minimised. Therefore, with this condition (46), the constants are evaluated

$$\frac{\partial V_{u1}}{\partial d_{11}} = 0, \quad \frac{\partial V_{u1}}{\partial d_{21}} = 0, \quad \frac{\partial V_{u2}}{\partial d_{21}} = 0, \quad \frac{\partial V_{u2}}{\partial d_{22}} = 0, \quad (46)$$

Fig. 9 shows percentage of linear deflection for PCD in the case of 0.53% error. Observably, increase of b reduces linear zone of diaphragm's response to pressure.

5. Conclusions: In this Letter, a new structure of diaphragm called 'piston coupled diaphragm' was studied. Based on the classical theory of plates, a deflection formula was derived. Then, sensitivity of a pressure sensor was shown and theoretical and simulation results were compared with each other. It was suggested that if surfaces of suspended electrode and diaphragm are equal, total sensitivity of diaphragm will triple. In addition, higher dimensions of electrode will directly increase sensitivity of PCD in comparison with simple one. Increase of sensitivity through enhancing surface of electrode will reduce measurable low threshold; this is a major advantage for sensitive sensors used for measuring millipascal pressures. The factors contributing to limitation of dynamic range are analysed and based on the error of nonlinear behaviour of simple diaphragms; a measure of linear range was developed for PCD.

6 References

- [1] Lin L., Yun W.: 'MEMS pressure sensors for aerospace applications'. IEEE Aerospace Conf., Aspen, CO, USA, 1998, vol. 1
- [2] Bogue R.: 'MEMS sensors: past, present and future', *Sens. Rev.*, 2007, **27**, 1, pp. 7–13
- [3] Beeby S.P., Stuttle M., White N.M.: 'Design and fabrication of a low-cost microengineered silicon pressure sensor with linearised output', *IEE Proc., Sci. Meas. Technol.*, 2015, **147**, 3, pp. 127–130
- [4] Bell D.J., Lu T.J., Fleck N.A., *ET AL.*: 'MEMS actuators and sensors: observations on their performance and selection for purpose', *J. Micromech. Microeng.*, 2005, **15**, (7), p. S153
- [5] Zhang Y., Howver R., Gogoi B., *ET AL.*: 'A high-sensitive ultra-thin MEMS capacitive pressure sensor'. Solid-State Sensors, Actuators and Microsystems Conf., 2011
- [6] Eswaran P., Malavizhi S.: 'MEMS capacitive pressure sensors: a review on recent development and prospective', *International Journal of Engineering and Technology (IJET)*, 2013, **5**, (3), pp. 2734–2746
- [7] Dowlatia S., Rezazadehb G., Afranga S., *ET AL.*: 'An accurate study on capacitive microphone with circular diaphragm using a higher order elasticity theory', *Lat. Am. j. solids struct.*, 2016, **13**, (4), p. 323
- [8] Ning F., Wei J., Qiu L., *ET AL.*: 'Three-dimensional acoustic imaging with planar microphone arrays and compressive sensing', *J. Sound Vib.*, 2016, **380**, pp. 112–128
- [9] Martin T.D., Jian L., Karthik K.: 'A Micromachined dual-backplate capacitive microphone for aeroacoustic measurements'. *Journal of Microelectromechanical Systems*, 2007, **16**, (6), pp. 1289–1302
- [10] Di Giovanni M.: 'Flat and corrugated diaphragm design' (Marcel Dekker, Handbook, New York, 1982)
- [11] Padron I., Fiory A.T., Ravindra N.M.: 'Introduction of embossed diaphragm in an integrated optical and electronic sensor', *Adv. Electroceram. Materials II*, 2008, **221**, pp. 195–204
- [12] Timoshenko S.P., Woinowsky-Krieger S.: 'Theory of plates and shells' (McGraw-Hill, USA, 1959), pp. 420–500
- [13] Wangsness R.K.: 'Electromagnetic fields' (Wiley-VCH, New Jersey, USA, 1986)
- [14] Oppenheim A.V., Willsky A.S., Hamid S., *ET AL.*: 'Signals and systems', vol. 2 (Prentice-Hall, Englewood Cliffs, NJ, 1983)
- [15] Beeby S.: 'MEMS mechanical sensors' (Artech House, 2004)